

# Morphological changes in PANi/PMMA-Blends during dispersion studied by SAXS

W. Lennartz<sup>a</sup>, T. Mietzner<sup>a</sup>, G. Nimtz<sup>a</sup> and B. Wessling<sup>b</sup>

<sup>a</sup>II. Physikalisches Institut, Universität zu Köln, Zùlpicher Str. 77, 50937 Köln, Germany

<sup>b</sup>Ormecon Chemie (Subsidiary of Zipperling Kessler & Co) Ammersbek, Germany

---

## Abstract

SAXS studies of polyaniline blends have been performed to investigate the mesoscopic morphology between 1 and 100 nm. It is concluded, that the molecules fold to crystals. These crystals are stacked to primary particles. At higher bulk conductivity the primary particles are more compact.

*Key words:* Polyaniline and derivates, Metal-insulator phase transitions, Structural phase transitions, Melt processing

---

Various studies of polyaniline (PANi) revealed that the protonated conducting form consists of a partially crystalline core [1] surrounded by an amorphous shell. The charge transport is determined by two effects: the conductivity of the metallic core and the hopping process through the non-crystalline barrier [2]. As we could show an increase of the conductivity is correlated with a decrease of the elemental cell volume in the metallic region [3]. It has been shown, that the melt dispersion of PANi in Polymethyl-methacrylat (PMMA) improves the conductivity of this blend strongly [5] and induces the "insulator-to-metal" transition [3]. Here we investigate how this behavior is correlated with changes in the PANi morphology. To observe possible morphological alterations caused by the melt dispersion process, we performed small-angle X-ray scattering experiments (SAXS) on two concentration series (528 and 578) of p-toluenesulfonic acid doped PANi dispersed in PMMA. The two series differ in their conductivity ( $\sigma_{528} \ll \sigma_{578}$ ) and the critical volume fraction  $f_c$  for the conductivity breakthrough (528:  $f_c = 8.5\%$ , 578:  $f_c = 4.8\%$ ). The dispersion process and sample preparation technique used are described elsewhere [3,4].

The SAXS experiments were performed using a Kratky-Kamera with a step scan detector and a slit-collimation system mounted to a Siemens rotating anode XP18 with CuK $\alpha$  radiation. The

observable scattering momentum transfer  $h = (4\pi/\lambda) \sin(\theta)$  was  $0.01$ - $5.9 \text{ nm}^{-1}$ . Background corrected SAXS patterns for the 528 Series are shown in Fig. 1. The SAXS-curves are divided into two parts: for  $h \leq 0.3 \text{ nm}^{-1}$  the typical small-angle broadening of the primary beam is obtained; in  $h > 0.3 \text{ nm}^{-1}$  a shoulder in the scattering curves is recognized, which is characteristic for a smeared peak.

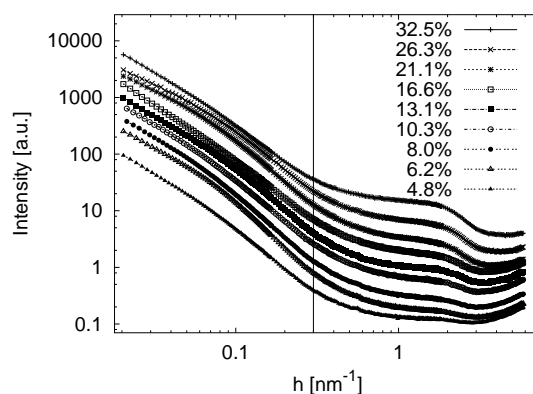


Fig. 1. SAXS-Curves of 528.

First we studied the peak. To obtain its position we desmeared our data according to [6]. The result for the samples with the highest concentration of each series is shown in Fig. 2. Sample 528 shows a slightly stronger pronounced re-

flex indicating that more particles are involved in the scattering process. According to Bragg's law, the lattice period has been determined to 3.45 nm for both blend series. Wide-angle X-ray analysis yields an estimated size of the crystalline core: perpendicular to the chain-direction, the crystalline areas are around 3 nm for pure 578, very close to our SAXS result. Therefore we associate the reflexes to the size of periodically stacked crystalline domains of individual PANi molecules.

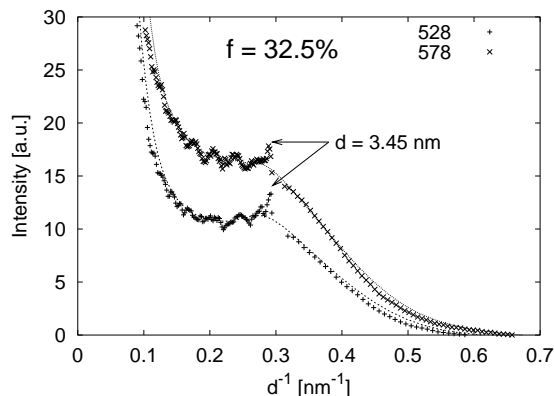


Fig. 2. Desmeared SAXS-pattern for 32.5% PANi..

Second, we studied the left side of Figure 1. In the PANi/PMMA dispersion it is expected to detect PANi particles consisting of various crystalline units. Hence for  $h < 0.3 \text{ nm}^{-1}$  we calculated size distributions for spherical particles using the Structure Interference Method [7,8]. The computations have been done for real space discretisation for the radius between 1 nm to 100 nm. The result is an appearing main structure in the region between 3 nm and 16 nm. At higher concentration and concurrently growing conductivity the size distribution shifts remarkably to smaller radii for both sample series. Center of gravity calculations from the distribution functions are shown in Fig. 3. Not only the particles within a series shrink with more PANi dispersed, but also the better conducting material starts with smaller particles even at low concentration. A second, less pronounced structure becomes visible around 25 nm.

Summarizing, we have found a substructure within the dispersed particles with a diameter around 3.45 nm, and the next bigger particles between 13 and 21 nm, depending on concentration and conductivity, and around 50 nm, respectively. The observations are in line with earlier TEM findings, where secondary particles between 50 and 100 nm, showing a finestructure, had been detected [9]. For interpretation, we consider:

- Emeraldine base particles in colloidal dispersion are smaller than those of the Emeraldine salt

(i.e., protonated PANi), the former being around 5 nm, the latter around 10 nm [10].

- Dielectric studies showed a metallic core of 8 nm, surrounded by 0.8 nm shell ( $\approx 10 \text{ nm}$ ).

A possible explanation could therefore be, that the primary particles (the smallest possible particle accessible in dispersion and the smallest particle with showing full PANi properties) of protonated PANi consist of about 8 molecules folded to form crystals, which associate to said primary particles of around 10 nm size, forming a homogeneous metallic core. The molecules and hence the particles will be compacted due to shear induced crystallization (the one leading to the "insulator-to-metal" transition), so that we find smaller particles with higher conductivity. In EB dispersions, we find isolated molecules since the particles do not have such a high surface tension.

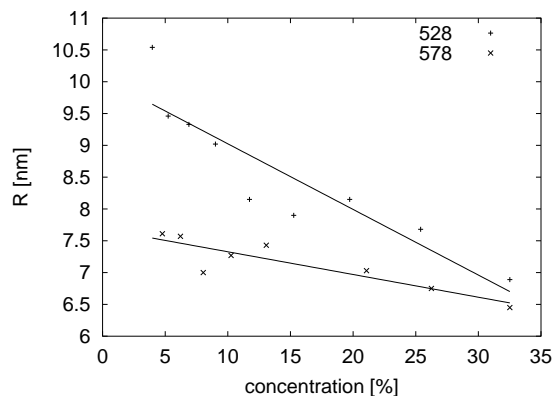


Fig. 3. Particle radii decrease with concentration.

## References

- [1] J.P. Pouget, M.E. Jozefowicz, A.J. Epstein, X. Tang, A.G. MacDiarmid, *Macromolecules* **24**, 770 (1991).
- [2] R. Pelster, G. Nimtz, B. Wessling, *Phys. Rev. B* **49**, 12718 (1994).
- [3] B. Wessling, D. Srinivasan, G. Rangarajan, T. Mietzner, W. Lennartz, *EPJ*, in press.
- [4] Zipperling Kessler & Co., US 5,567,355 (priority 1987).
- [5] C.K. Subramaniam, A.B. Kaiser, P.W. Gilberd, C.J. Liu, B. Wessling, *Solid State Commun.* **97**, 235 (1996).
- [6] A. Guinier, G. Fournet, *Small Angle Scattering of X-Rays*, Wiley (New York), (1955).
- [7] H.G. Krauthäuser, *Physica A* **211**, 317 (1994).
- [8] H.G. Krauthäuser, G. Nimtz, *Journal of Molecular Structure* **383**, 315 (1996).
- [9] B. Wessling in: *Handbook of Nanostructured Materials and Nanotechnology*, Vol. 5: Organics, Polymers, and Biological Materials, Academic Press, Ed. by Hari Singh Nalwa, (2000).
- [10] B. Wessling, *Adv. Mater.* **5**, **4**, 300, (1993).